Energy level alignment of C$_{60}$/Co using x-ray and UV photoelectron spectroscopy

# Energy level alignment of $C_{60}$/Co using x-ray and UV photoelectron spectroscopy

**J H Seo[1], S J Kang[2], C Y Kim[1], K-H Yoo[1] and C N Whang[1,3]**

[1] Institute of Physics and Applied Physics, Yonsei University, Seoul 120-749, Korea
[2] Department of Materials Science and Engineering, University of Illinois at Urbana Champaign, Urbana, IL 61801, USA

E-mail: cnwhang@yonsei.ac.kr

**Abstract**
The energy level alignment at the interface between fullerene ($C_{60}$) and Co has been determined by x-ray and ultraviolet photoelectron spectroscopy. To investigate the interfacial electronic structure, a $C_{60}$ layer was deposited on a clean Co surface in a stepwise manner. The measured onset of the highest occupied molecular orbital energy level was at 1.54 eV from the Fermi level of Co. The vacuum level was shifted 0.41 eV toward lower binding energy with the additional $C_{60}$ layers, which means that an interface dipole exists at the interface between $C_{60}$ and Co. The C 1s spectra show that band bending occurs at the interface between $C_{60}$ and Co. These results indicate that the barrier height of the hole injection from Co to $C_{60}$ is 1.14 eV, which is a smaller value than that for electron injection (1.46 eV).

## 1. Introduction

Organic semiconductors (OSEs) are a relatively new field of electronic materials that are revolutionizing important technological areas including information display and large area electronics. OSEs have many advantages, such as low process cost, device flexibility, and the simplicity of thin film device fabrication, which have helped to attract many researchers to study organic semiconductor devices [1]. Many useful developments in materials and devices for OSEs have been reported in previous studies [2–4]. From these, we expect to see organic semiconductors such as pentacene, fullerene ($C_{60}$), and several other organic materials replacing the traditional inorganic semiconductors in the near future. However, attempts to fabricate organic spintronics have been fewer than those to obtain organic semiconductor devices (organic thin film transistors, organic light emitting devices, and so on).

Several organic materials are used to fabricate organic spintronics [5]. Pentacene, $C_{60}$, and 8-hydroxyquinoline aluminium (Alq$_3$) are representative organic materials that are used

---

[3] Author to whom any correspondence should be addressed.

in organic magnetic semiconductor devices. In particular, mixed $C_{60}$–Co films have attracted considerable attention due to their promising magnetic properties. The $C_{60}$–Co nanocomposite materials prepared properly have revealed the characteristic of giant magnetoresistance (GMR) [6, 7]. Xiong *et al* have reported that spin polarized carrier injection, transport, and detection, which are the main ingredients of spintronics, can be successfully achieved using $\pi$-conjugated OSEs (Alq$_3$) [8]. Bergenti *et al* have reported that spin polarized materials can successfully replace conventional electrodes in organic light emitting diodes (OLEDs) [9]. Recently, Meruvia *et al* have produced TFTs by evaporating $C_{60}$ as the emitter in magnetic metal-based transistors [10]. Although organic spintronic devices, associating organic semiconductors and magnetic materials, have been investigated by several researchers [8–11], there have been fewer attempts to understand the mechanism of these devices.

If the advantages of the $C_{60}$/Co interface are considered, the electronic structure of $C_{60}$/Co is important because the electronic structure directly affects charge transport in organic application devices [12].

In this paper, we analysed the valence band spectra of the $C_{60}$/Co interface obtained from ultraviolet photoelectron spectroscopy (UPS). And the band bending (charge redistribution) was investigated by using x-ray photoelectron spectroscopy (XPS). An energy level diagram is summarized, which contains the electron injection barrier height and interface dipole.

## 2. Experimental details

The XPS and UPS measurements were performed in an ultrahigh vacuum (base pressure $1 \times 10^{-10}$ Torr) condition by using a PHI 5700 spectrometer equipped with Al K$\alpha$ (1486.6 eV) and a He I (21.2 eV) discharge lamp. The sample was prepared in a preparation chamber, which was connected to the XPS and UPS measurement chamber. A clean Co surface was obtained by sputtering a commercial Co foil (99.99%) to remove the residual oxides and carbon contaminations. After cleaning the Co substrate, $C_{60}$ was deposited on the clean Co in a stepwise manner to investigate the interfacial electronic structure. The deposition rates for $C_{60}$ were kept at 0.01 nm s$^{-1}$, and the nominal thickness was monitored with a calibrated quartz thickness monitor. During the deposition, the pressure of the preparation chamber was maintained at $1.4 \times 10^{-9}$ Torr. After each deposition of $C_{60}$, the valence band, C 1s, O 1s, and Co 2p spectra were immediately collected at a sample bias of $-15$ V in order to separate the sample and the analyser high binding energy cut-off.

## 3. Results and discussion

The He I UPS spectra of the interface formed by deposition of $C_{60}$ on Co are presented in figures 1 and 2. The spectra were collected along the surface normal direction with a photon incidence angle of 30°. From the sample with a $C_{60}$ layer, the Fermi level was decided and all other spectra were plotted with respect to the Fermi level. The valence band spectra of $C_{60}$ with thicknesses of 0, 0.2, 0.4, 0.8, 1.6, 3.2, 6.4, and 25.6 nm are shown in order, with the spectrum for a zero thickness being the Co valence band spectrum. The spectra obtained from $C_{60}$/Co obviously display the HOMO level. On depositing $C_{60}$, the emission from the Co substrate becomes suppressed, and the spectrum is changed to that of $C_{60}$. The shift of the HOMO onset of $C_{60}$ from the Fermi level of Co gives the relative position of the HOMO from the Fermi level of Co. The HOMO level of $C_{60}$ appeared slightly at a $C_{60}$ thickness of 0.2 nm on Co, and the HOMO level was clearly seen at a $C_{60}$ thickness of 3.2 nm. From the sample with a thick $C_{60}$ layer (25.6 nm), we decided that the HOMO onset of the $C_{60}$ layer was located at 1.54 eV below the Co Fermi level.
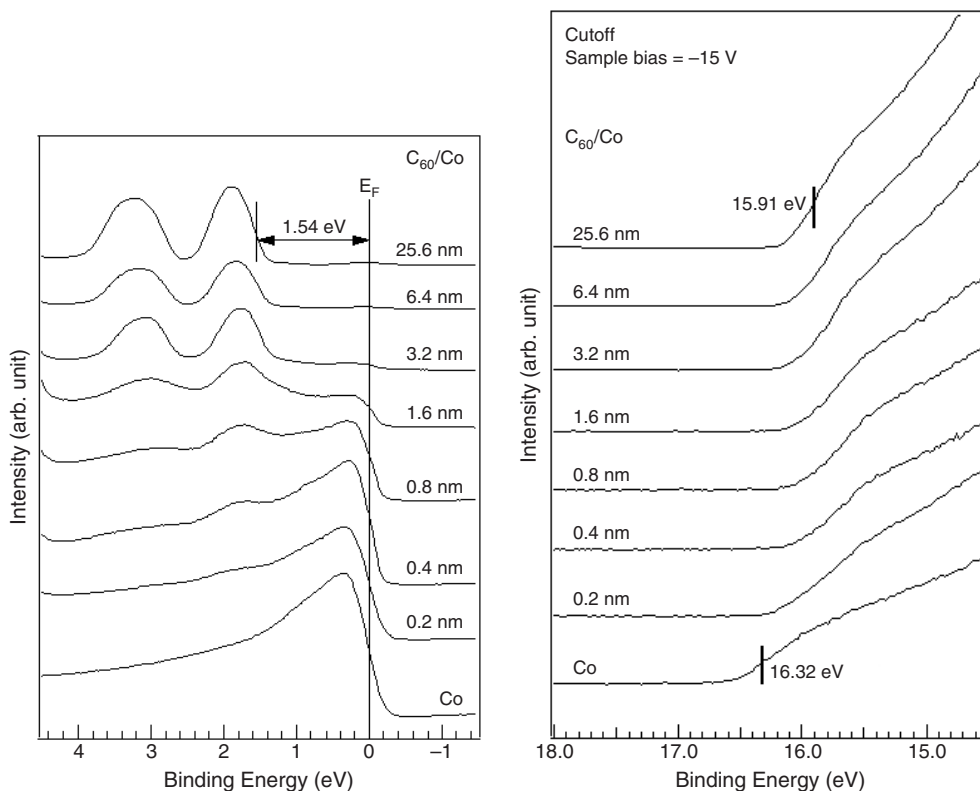
**Figure 1.** UPS spectra measured immediately after each C$_{60}$ layer deposition with a sample bias of $-15$ V. Low energy edges of the HOMO of the C$_{60}$ layers and Fermi level of a Co layer are shown with vertical lines.

**Figure 2.** UPS spectra in the high binding energy cut-off region of C$_{60}$ are shown for various C$_{60}$ thicknesses. The intensity is normalized to allow better comparison between spectra.

    The He I UPS spectra in the high binding energy region of clean Co and of 0.2, 0.4, 0.8, 1.6, 3.2, 6.4, and 25.6 nm thick C$_{60}$ layers on Co are shown in figure 2. The vacuum levels of the samples were determined by linear extrapolation of the cut-off of secondary electrons on the high binding energy side of the UPS spectra. The abscissa is the binding energy relative to the Fermi level of the Co layer. A $-15$ V sample bias was applied to separate sample and analyser spectral cut-offs and to increase the emission strength of the secondary cut-off. One half of the total broadening is 0.1 eV for the analyser resolution (as determined from the width of the Fermi edge). As the C$_{60}$ was deposited on the Co, the high binding energy cut-off moved to lower binding energy. At a sufficient coverage of 25.6 nm, the high binding energy cut-off has shifted to lower energy by 0.41 eV. This means that the vacuum level is higher compared to that of the Co. Compared with our previous results, the interface of C$_{60}$ on Au (the work function of Au is 5.2 eV) shows that the vacuum level was shifted 0.54 eV from that of Au toward higher binding energy with additional C$_{60}$ layers [13]. This shift in the high binding energy cut-off is attributed to an interface dipole between C$_{60}$ and Co. The redistribution of electrons at the interface between C$_{60}$ and Co occurs as C$_{60}$ is deposited on Co.

    Figure 3 shows the results of the XPS measurements. Figure 3 shows the C$_{60}$ overlayer related C 1s emission lines and figure 4 shows the Co 2p lines. There was no contamination
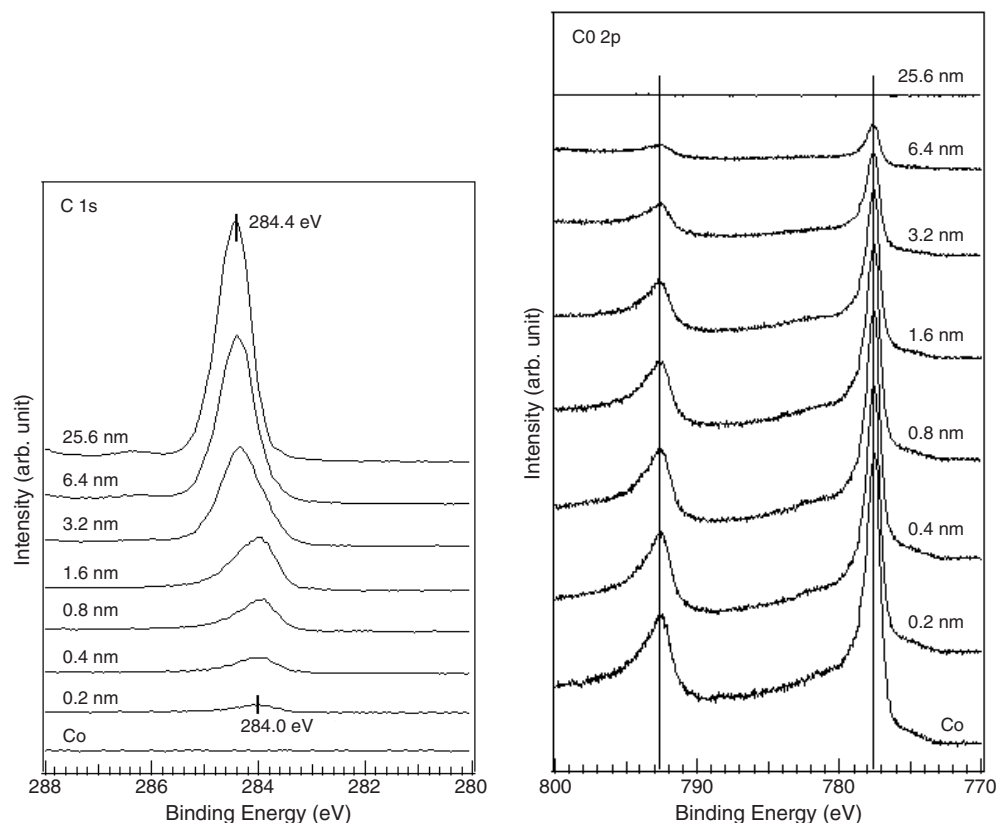
**Figure 3.** XPS spectra of the C 1s core levels as a function of $C_{60}$ coverage on the Co substrate layer.

**Figure 4.** XPS spectra of the Co 2p core levels.

by carbon on the pristine Co surface. The subsequent spectra were measured after deposition steps from 0.2 to 25.6 nm. As the deposited amount increases the C 1s emissions increase in intensity, while Co 2p emissions become attenuated due to the formation of the $C_{60}$ overlayer. The total C 1s peak shift was 0.4 eV toward high binding energy after a sufficient coverage of $C_{60}$ (25.6 nm) had been achieved. The lack of a remarkable characterization change in the C 1s peak implies the absence of chemical bonds at the $C_{60}$ and Co interface, which means that the magnitude of the band bending at the interface is 0.4 eV due to the charge redistribution. In figure 4, we also investigated the core level spectra of Co and found no significant changes in the peak shape. The peak position of Co 2p did not change with the deposition of $C_{60}$ on the Co surface. Therefore, we suggest that the Co surface remained chemically intact due to the organic overlayers, resulting in no band bending in the Co region.

From figures 1–4, we can obtain the interfacial electronic structure, between $C_{60}$ and Co. The ionization potential of $C_{60}$ was obtained by using

$$\text{Ionization potential} = h\nu - \text{cut-off} + E_{\text{HOMO}}. \tag{1}$$

$h\nu$ indicates the photon energy of 21.2 eV, 'cut-off' means the high binding energy cut-off, and $E_{\text{HOMO}}$ means the onset of the HOMO level. According to equation (1), the ionization potential of $C_{60}$ was 6.83 eV. The difference between the Fermi level of Co and the HOMO onset of $C_{60}$ was 1.54 eV. By using 2.6 eV as the band gap of $C_{60}$ [13], the energy of the LUMO of $C_{60}$ can
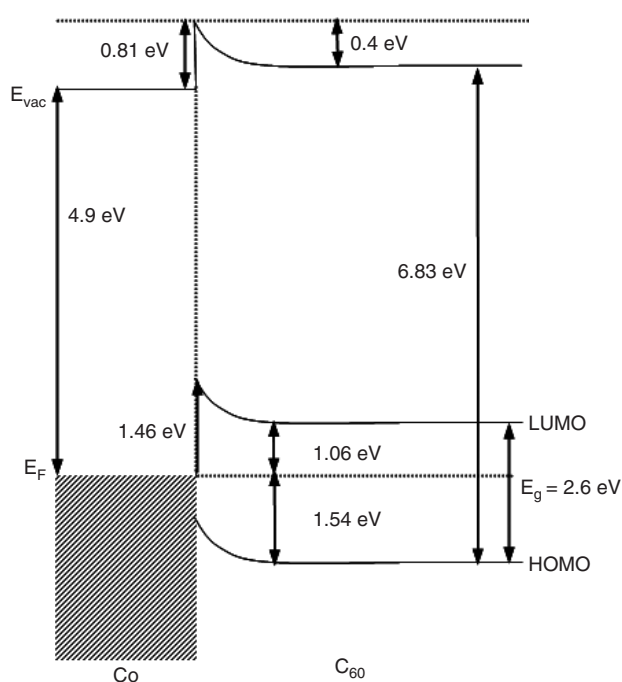
**Figure 5.** Energy level diagram of the $C_{60}$/Co interface.

be determined. Therefore, the barrier height for electron injection from Co to $C_{60}$ is 1.46 eV. In addition, the vacuum level of $C_{60}$ is shifted 0.41 eV from that of Co toward low binding energy. As we know from the C 1s spectra of $C_{60}$, band bending occurred. Therefore, the magnitude of the interface dipole is 0.81 eV. The above results are summarized in figure 5 where the energy level alignment of the $C_{60}$/Co interface is shown.

## 4. Conclusions

We obtained the electronic structure of the $C_{60}$/Co interface by using x-ray and ultraviolet photoelectron spectroscopy. $C_{60}$ was deposited in several steps starting from the submonolayer up to the sufficient coverage of 25.6 nm thickness on a clean Co surface. The highest occupied molecular orbital energy onset was measured as 1.54 eV from the Fermi level of Co, and the shift in the vacuum level was 0.41 eV toward lower binding energy. Moreover, band bending (0.4 eV) occurred at the $C_{60}$/Co interface, and the interface dipole was 0.81 eV. This observation provides a complete picture of the electronic structure of the $C_{60}$/Co interface. These results indicate that the barrier height of the hole injection from Co to $C_{60}$ is 1.14 eV, which is smaller than the barrier height of electron injection (1.46 eV).

## Acknowledgments

## References

[1] Kuwahara E, Kubozono Y, Hosokawa T, Nagano T, Masunari K and Fujiwara A 2004 *Appl. Phys. Lett.* **85** 4765
[2] Haddon R C, Perel A S, Morris R C, Palstra T T M, Hebard A F and Fleming R M 1995 *Appl. Phys. Lett.* **67** 121
[3] Saito R, Dresselhaus G and Dresselhaus M S 1998 *Physical Properties of Carbon Nanotubes* (London: Imperial College Press) pp 35–225
[4] Lavrentiev V, Abe H, Yamamoto S, Naramoto H and Narumi K 2002 *Physica* B **323** 303
[5] Wolf S, Awschalom D D, Buhrman R A, Daughton J M, von Molnár S, Roukes M L, Chtchelkanova A Y and Treger D M 2001 *Science* **294** 1488
[6] Baibich M N, Broto J M, Fert A, Nguyen Van Dau F, Petroff F, Eitenne P, Creuzet G, Friederich A and Chazelas J 1986 *Phys. Rev. Lett.* **61** 2472
[7] Moodera J S and Nassar J 1999 *Annu. Rev. Mater. Sci.* **29** 381
[8] Xiong Z H, Wu D, Valy Vaedeny Z and Shi J 2004 *Nature* **427** 821
[9] Bergenti I, Dediu V, Arisi E, Mertelj T, Murgia M, Riminucci A, Ruani G, Solzi M and Taliani C 2004 *Org. Electron.* **5** 309
[10] Meruvia M S, Munford M L, Hümmelgen I A, da Rocha A S, Sartorelli M L, Pasa A A, Schwarzacher W and Bonfim M 2005 *J. Appl. Phys.* **97** 026102
[11] Bergenti I, Dediu V, Arisi E, Mertelj T, Murgia M, Riminucci A, Ruani G, Solzi M and Taliani C 2004 *Org. Electron.* **5** 309
[12] Kang S J, Yi Y, Kim C Y and Whang C N 2005 *J. Korean Phys. Soc.* **46** L760
[13] Kang S J, Yi Y, Kim C Y and Whang C N 2005 *J. Korean Phys. Soc.* **46** 1148